Performance and Reliability of Widely Tunable Laser Diodes

T. Wipiejewski, Y. A. Akulova, G. A. Fish, P. C. Koh, C. Schow, P. Kozodoy, A. Dahl, M. Larson,
M. Mack, T. Strand, C. Coldren, E. Hegblom, S. Penniman, T. Liljeberg, L. A. Coldren
Agility Communications, Inc., 600 Pine Ave, Santa Barbara, CA 93117
Phone: (805) 690-1781, Fax: (805) 690-1855
torsten@agility.com

Abstract

We are manufacturing widely tunable laser diodes based on an integrated single chip design. The sampled-grating distributed Bragg reflector (SG-DBR) laser is monolithically integrated with a semiconductor optical amplifier (SOA). The continuous wave (cw) output power of the fully packaged device is more than 20mW over the entire C-band with low noise figures and a high side-mode suppression ratio of over 40dB. Devices are made for L-band operation as well. The devices are well suited for long-haul and ultra-long-haul DWDM optical transport systems.

For metro type applications we developed an EML-type device with a SG-DBR widely tunable laser monolithically integrated with an SOA and an electro-absorption modulator (EAM) based on the Franz-Keldysh effect. The operating speed is 2.7Gbit/s for OC-48 systems including forward error correction (FEC). The time averaged output power is in excess of 5dBm over the 40nm C-band tuning range. The extinction ratio is larger than 10dB. Error free transmission over more than 350km of standard single mode fiber is demonstrated. Wavelength switching is accomblished in less than 10ms which is limited by the control electronics.

The monolithically integrated widely tunable SG-DBR lasers show excellent reliability and environmental stability results. After testings hundreds of devices over several thousands of hours a long wear-out lifetime of over 350 years has been inferred with a very low failure rate of less than 100FITs over the normal operating lifetime. The results indicate no reliability penalty for wavelength tunability compared to standard fixed wavelength DFB lasers.

Introduction

Modern DWDM optical communication systems can employ more than 100 channels over a single fiber. Most systems operate in the C-band (1528 – 1568nm). Some systems extend the operating wavelength range to the L-band (1568 – 1610nm). The most common channel spacing is 50GHz with some systems operating on 25GHz channel spacing.

Figure 1 shows a schematic of the optical layer of a typical DWDM system. The light of a cw-fixed wavelength laser is modulated by an external high-speed modulator. Many laser channels with different wavelength are combined in an AWG and boosted by a fiber amplifier before being launched into a single mode fiber. After some in-line amplification the light is split according to the different channels, detected and amplified in the receiver side of the optical transmission system.

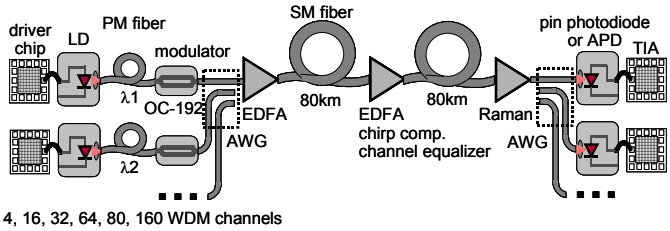

Fig. 1: DWDM long-haul optical transmission system.

Fixed wavelength lasers are made and individually selected for a specific wavelength in a DWDM system according to the wavelength assignment of the ITU grid. Thus, for an 80 channel system 80 different lasers each with an individual product code are required. It is easy to see how difficult the inventory management for hundreds of components can be. Also for sparing purposes linecards need to be stored for each wavelength.

Widely tunable lasers are capable of generating every optical channel in the entire C-band or L-band. Thus, one tunable laser can replace any fixed wavelength laser in a DWDM system. Since only one product code is required, the inventory and sparing management is greatly simplified and the cost of stored inventory is drastically reduced.

The next generation of re-configurable optical networks [1], [2] require tunable lasers as light sources. Re-configurable networks offer a higher degree of flexibility for capacity allocation. This is expected to become an important feature, especially in the metro space where traffic patterns are more fluid.

For metro applications we developed a widely tunable laser with an integrated modulator [3], [4], [5]. The monolithic integration scheme reduces power consumption compared to the discrete solution shown in Fig. 1, because there is no optical coupling loss at the fiber-device interfaces. The integration [6] also reduces size and cost, since we are using only one package instead of two for the discrete solution.

This paper describes the performance and reliablity of widely tunable SG-DBR laser with and without an integrated electro-absorption modulator. The devices are becoming key components for the next generation of optical networks.

Tunable Laser Design

The tunable laser design shown in Fig. 2 contains a sampled-grating distributed Bragg reflector (SG-DBR) laser integrated with a semiconductor optical amplifier (SOA) and an electro-absorption modulator based on the Franz-Keldysh effect.

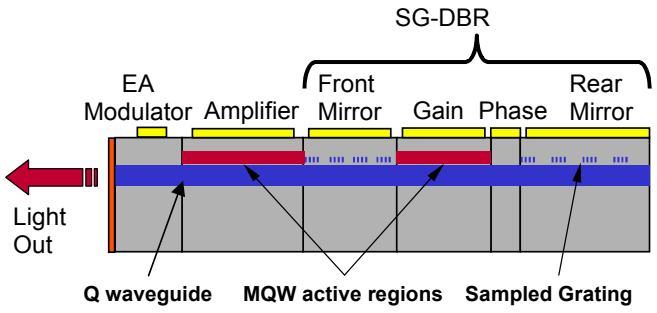

Fig. 2: Design of a widely tunable laser with sampled-grating distributed Bragg reflectors (SG-DBR) integrated with a optical amplifier (SOA) and an electro-absorption modulator.

The SG-DBR laser [7], [8] includes a gain and a phase section positioned between two "sampled grating" distributed Bragg reflectors. The additional periodicity of the DBRs transforms the reflectivity spectra of the mirrors into a comb of reflectivity peaks centered on the Bragg wavelength. The spacing between adjacent peaks is inversely proportional to sampling period. The gratings are defined holographically and sampled using standard lithography. The front and back mirrors of the laser are sampled at different periods such that only one of their multiple reflection peaks coincides at a time. This creates a Vernier effect and enables a wide wavelength tuning range. Introducing a small index change in one mirror relative to the other causes adjacent reflectivity maxima to come into alignment, shifting the lasing wavelength a large amount for small index change. Continuous tuning between the reflectivity maxima is obtained by tuning both mirrors simultaneously. Biasing of the phase section fine-tunes the effective Fabry-Perot cavity mode into alignment with the maximum reflectivity of the mirrors. The tuning range of a SG-DBR laser is defined by the repeat mode spacing and can be designed to exceed the tuning range of a conventional DBR laser by a factor of ten. Optimization of the device for C- or L-band operation is accomplished by alignment of the gain spectra and Bragg wavelength of the holographically defined grating within the respective band.

The integrated SOA compensates on-state modulator loss and cavity losses caused by free carrier absorption in the tuning sections. It also enables the output to be blanked while the laser is tuned and can be used as a variable optical attenuator (VOA). The integration of the laser and SOA active regions with the tuning and modulator sections of the device has been accomplished by using an offset quantum-well structure. In this simple integration technology the active region of the modulator uses the same bulk quaternary waveguide as the tuning sections of the laser. The Franz-Keldysh effect in the bulk waveguide material provides a larger spectral bandwidth as compared to the quantum-confined Stark effect. The composition of the bulk waveguide can be optimized to achieve high tuning efficiency for the laser and a target extinction ratio for the modulator over the required wide spectral bandwidth.

The high power cw tunable laser design is based on the same structure, but does not employ the modulator section. The six section EML chip combines light generation, wavelength tuning, light amplification and leveling, and light modulation in a single device. The chip is an example of the highest level of integration in the field of optoelectronics.

Packaging and Control Electronics

The laser chip is mounted in a 24-pin butterfly package with co-planar RF input lines. The butterfly package contains a thermo electric cooler, the coupling optics, an optical isolator, and a wide spectral range wavelength locker. The butterfly is assembled with control electronics into an MSA (multi source agreement) transmitter package. The output fiber is standard single mode (SM) for the EML transmitter and polarization maintaining (PM) fiber for the cw laser product. Figure 3 shows the new package for the 20mW cw laser transmitter. The outer dimensions are 2.9inches long by 2inches wide. The height is 0.52inches. The EML package is the same style, but slightly longer (3.9inches).

Fig. 3: Tunable laser transmitter package for 20mW output power and full C-band tuning range contains butterfly laser package and laser control electronics.

The widely tunable laser requires current control of the five sections of the device. The EML transmitter contains the additional bias and RF amplitude control for the modulator section. Output power and wavelength are control by

electronic feedback loops. The output power is maintained in reference to an internal monitor photodiode. The etalon signal of the wavelength locker is fed back to the phase section of the laser to stabilize the emission wavelength. The widely tunable transmitter assembly can be calibrated for 25 or 50 GHz channel spacing by adjusting the set points for the locker. Implementation of power control using the integrated SOA allows beam blanking to –30 dBm during wavelength switching and a variable optical attenuator function with a dynamic range in excess of 10 dB. Figure 4 illustrates the various feedback and control loops.

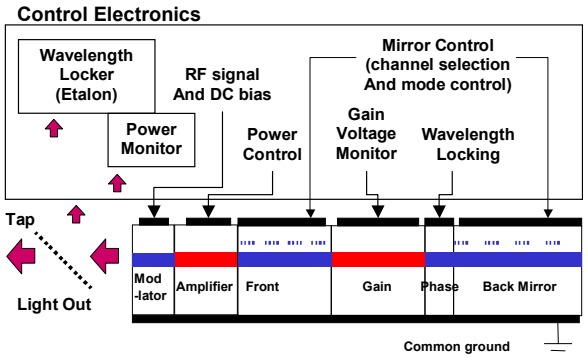

Fig. 4: Tunable laser transmitter feedback loops to control power, wavelength, and phase.

In addition to power and wavelength control we also implemented a mode control in the feedback loops of the tunable laser. The gain-voltage signal of the active section is used to stabilize the lasing mode in the center of the mirror-current mode map [9], [10].

CW Performance

Figure 5 exhibits the fiber coupled output power of the laser for the C- and L-band, respectively.

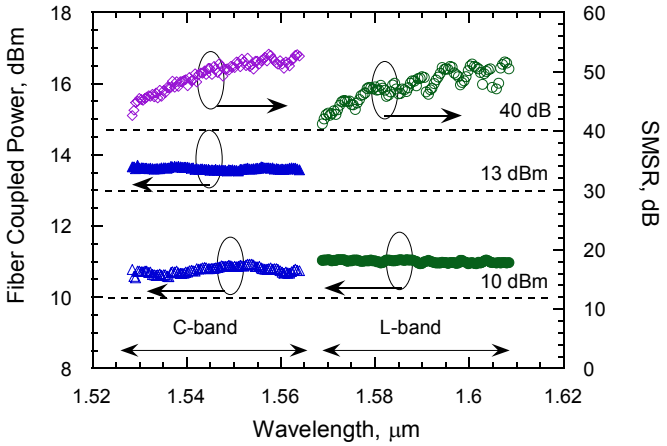

Fig. 5: Fiber coupled cw output power and side-mode suppresion ratio (SMSR) across C- and L-band.

More than 10dBm of cw power are available for operation in either wavelength range. For C-band operation the output power level has also been adjusted to 13dBm. Typical operation conditions for the 20 mW cw source are I_{gain} = 150 mA, I_{FM} and I_{BM} below 30 and 50 mA, respectively, and I_{SOA} below 150 mA.

The power is calibrated and stabilized according to the feedback scheme described above. 90 channels of the ITU grid can be selected for transmitters employing 50GHz channel spacing. For 25GHz channel spacing the number of selectable channels increases to 180. The side-mode suppression ratio SMSR of the tunable laser is greater than 40dB in both C- and L-band as indicated in Fig. 5.

The low noise figure of the laser is also confirmed in the RIN and linewidth data displayed in Fig. 6.

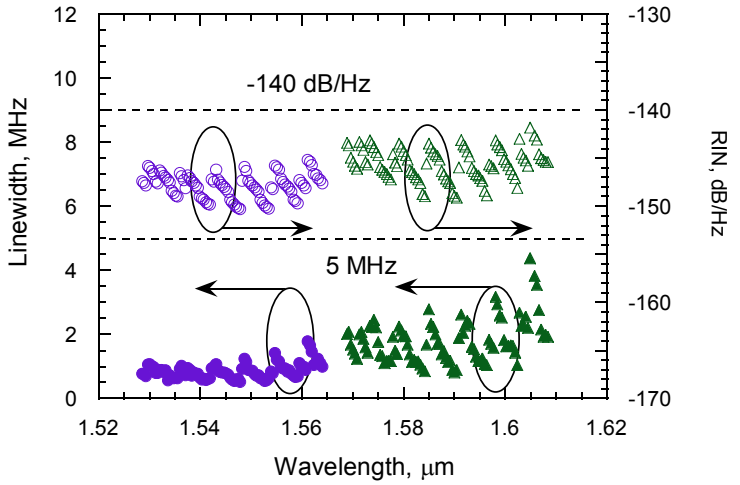

Fig. 6: RIN and linewidth for high power tunable laser across C- and L-band, respectively.

The linewidth of the integrated SG-DBR-SOA laser was measured using a coherent optical frequency discriminator technique [11]. The linewidth and RIN are inversely proportional to laser power and hence have periodic dependence on wavelength due to change in the mirror loss under tuning. The linewidth remains below 5MHz across the 40nm tuning range in C- and L-band, respectively. The averaged RIN within the 100MHz to 10GHz frequency range is less than –140dB/Hz.

Transmission Characteristics

The high speed performance of the EML is demonstrated in the eye diagrams of Fig. 7. The 2.5Gbit/s eyes are clean and wide open at the various wavelengths between 1528nm and 1560nm. The eye diagrams are shown with a SONET OC-48 mask with 25% margin. The receiver employs a 4th order Bessel-Thompson filter. The data pattern is pseudo random 2^{31}-1. The EML exhibits the same performance in applications including forward-error correction (FEC) that require a higher bit rate of 2.7Gbit/s.

Maintaining a low and uniform chirp is key for achieving uniform transmission performance of the integrated transmitter over wide wavelength range. The transient chirp and extinction ratio (ER) characteristics of EA-modulators are strongly dependent on the detuning between the lasing and absorption-edge wavelengths. Previously we have demonstrated that the detuning and hence ER and chirp can

be simultaneously controlled by adjusting the *dc* bias on the modulator section [12].

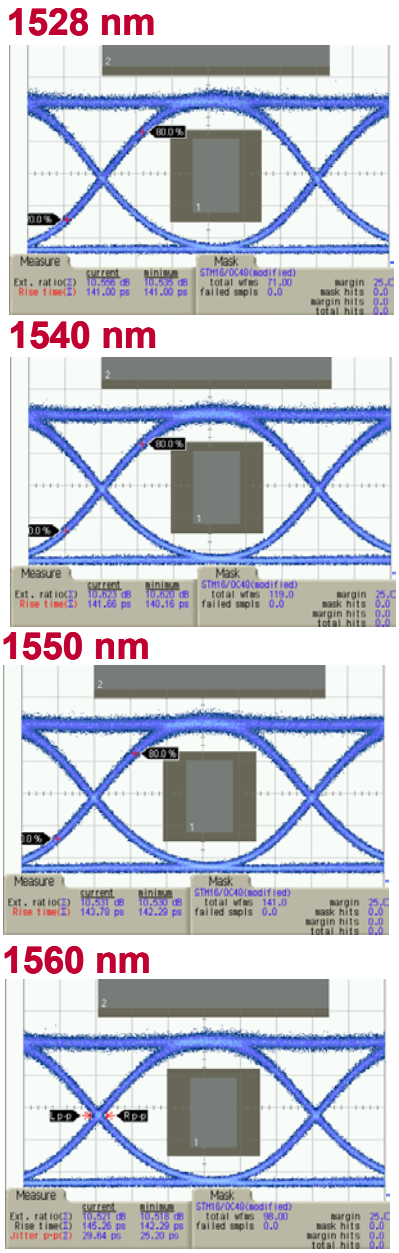

Fig. 7: Eye diagram of the EML transmitter running at 2.5Gbit/s at various wavelengths across the C-band. The SONET OC-48 mask indicates a 25% margin over the SONET spec.

A uniform, high *RF* extinction ratio (>10 dB) and low chirp (<0.2 A) over a wide spectral bandwidth were achieved by calibrating the *dc* bias and the modulation voltage settings for the modulator driver. Figure 8 shows the RF extinction ratio and the time averaged output power for the EML operating at 2.5Gbit/s over the entire C-band. The modulator driver circuit is integrated into the tunable laser transmitter product. Under modulation a fiber-coupled time-averaged power of 5 dBm is maintained across C-band by closed loop control using the integrated SOA.

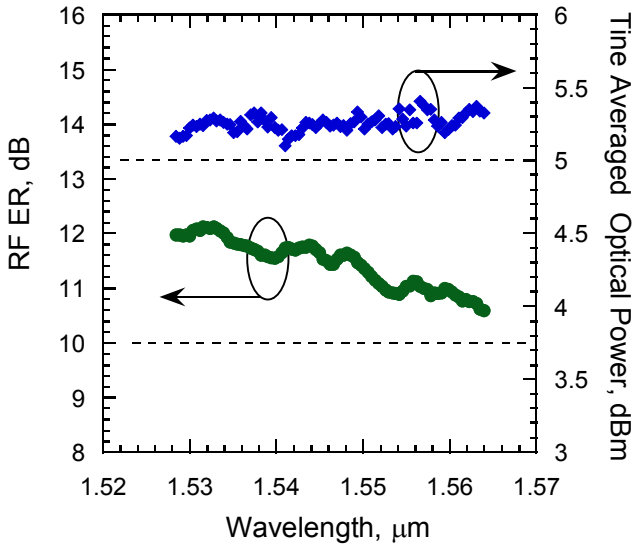

Fig. 8: RF extinction ratio (ER) and time averaged output power for EML operating at 2.5Gb/s across the C-band.

The fiber transmission test bed consists of the SG-DBR-SOA-EA transmitter followed by spans of conventional single mode fiber (SMF). The input power into the fiber spans was 3 and 7dBm for the first and consecutive spans, respectively. A tunable band pass filter was used after the final span to remove amplified spontaneous emission (ASE) noise. The power and wavelength control loops were engaged during the measurements and had no effect on transmission performance.

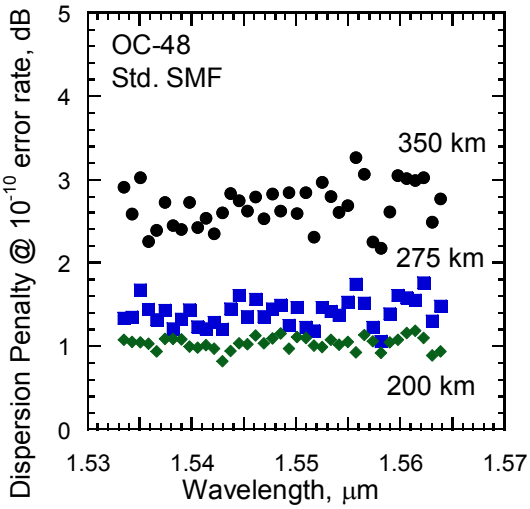

Fig. 9: Dispersion penalty at 10^{-10} errors/s error rate for 200, 275, and 350 km of standard SMF for 38 ITU channels sampled across C-band.

Figure 9 shows the dispersion penalty (DP) at 10^{-10} errors/s error rate for 38 ITU channels sampled across the C-band for 200, 275, and 350km of standard SMF. The short wavelength range for this measurement was limited to 1533nm by the tunable bandpass filter. The measured DP does not exhibit a significant wavelength dependence confirming the robustness of the EA-modulator chirp control over the wide tuning range.

Reliability of Widely Tunable SG-DBR Lasers

In order to assess the reliability of the SGDBR lasers, accelerated aging experiments were conducted on greater than 150 burned-in, screened devices from the Agility manufacturing line. Several temperature and current overstresses were applied to the devices for extended periods of time to ascertain the degradation rate as a function of current and temperature. Figure 10 shows an example of a stress matrix to assess mirror aging.

		Current Stress		
Temperature Stress		3x use	4x use	7x use
	50ºC			X
	75ºC			X
	100ºC			X
	96ºC		X	
	100ºC	X		

Fig. 10: Stress matrix to assess mirror aging. Sample size is 140 devices from 5 production wafers.

As the SG-DBR laser performance varies with channel, devices were calibrated at each measurement point in time, yielding the changes in the tuning currents to obtain the same channel over time. The updated calibration was then used to measure changes in other parameters such as threshold current and output power at multiple channels representing the extrema of calibrated currents and wavelength.

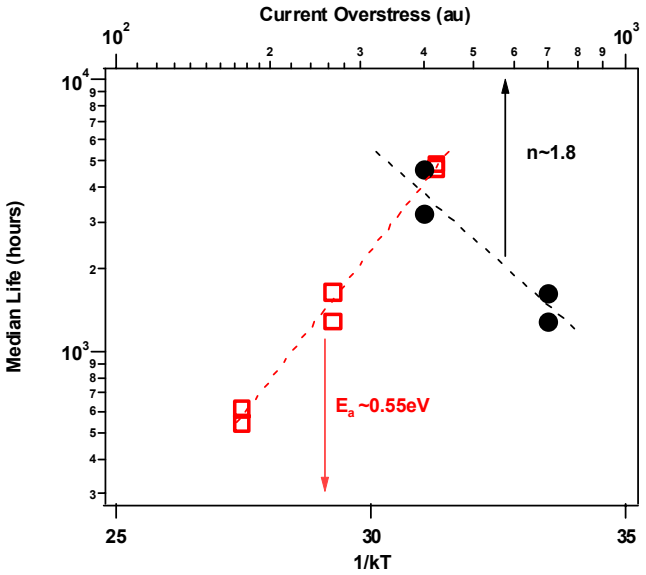

Fig. 11: Determination of tuning section acceleration factors in accelerated aging experiments. Data points are the median values for all of the parts at the particular aging stress. Least squares fitting yields an activation energy of E_a ~0.55eV and current acceleration exponent of n ~1.8.

The failure criteria used to determine tuning section life was set conservatively to ensure mode hop free operation even in the presence of degradation processes that are not accelerated during the accelerated life test, but may nevertheless occur during field deployment of the device including high and low temperature storage or mechanical/environmental stressing.

In order to predict the failure distribution at normal use conditions, the temperature and current dependent acceleration factors were determined by performing a two dimensional least squares fit to the median degradation rate at each stress condition. The aging data was fit to the following model:

$$aging\ rate \propto I^{-n} e^{\frac{-E_a}{kT}}$$

where I is the current, n the current acceleration factor, k the Boltzmann constant, T the absolute temperature, and E_a the activation enery. Figure 12 shows the median mirror aging rates, plotted versus temperature and current. A least squares fit to the data yields a thermal activation energy E_a of approximately 0.55eV and a current acceleration exponent n of approximately 1.8.

Using the acceleration factors to predict the lifetimes at operating conditions yields the cumulative failure distribution plotted in Fig. 12. The distribution was fit to the standard lognormal failure distribution for the purpose of calculating the instantaneous failure rate (in FITs). The failure rate due to passive tuning section wear out remains below 1 FIT over the expected useful life (~20 years).

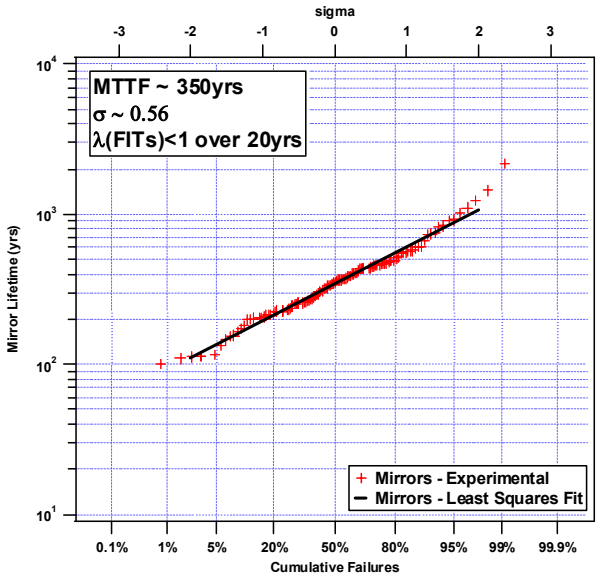

Fig. 12: Stress matrix to assess mirror aging. Sample size is 140 devices from 5 production wafers.

The accelerated aging data demonstrates that SG-DBR tuning sections can provide highly reliable operation over the anticipated useful life. As the lifetime of the SG-DBR laser depends not only on the tuning sections but the active sections, acceleration factors and failure rates for the active sections have also been determined. The data yields activation energies and current acceleration exponents very similar to the passive sections, which is not surprising, as the different sections are made from essentially the same materials by the

same processes. As the active sections are driven with higher currents than the tuning sections, the active section median life is slightly shorter than that of the tuning sections. However, adding the active and tuning failure rates results in a low total wear out failure rate that remains less than 100 FITs over the useful life of the device. These results show significant improvement compared to previous publications [13], [14], [15], [16].

Electro-Absorption Modulator Reliability

The reliability testing of the electro-absorption modulator (EAM) section of the EML devices was performed at elevated temperatures and high photocurrent stress levels. The ambient temperatures were chosen between 100°C and 175°C. The current levels were varied between 1.25 times to 2.25 times normal use currents. No degradation of device performance was observed over sereral thousands of hours of high stress aging. Figure 13 shows the measured change of extinction ratio for 56 devices running under different stress conditions for over 2500h.

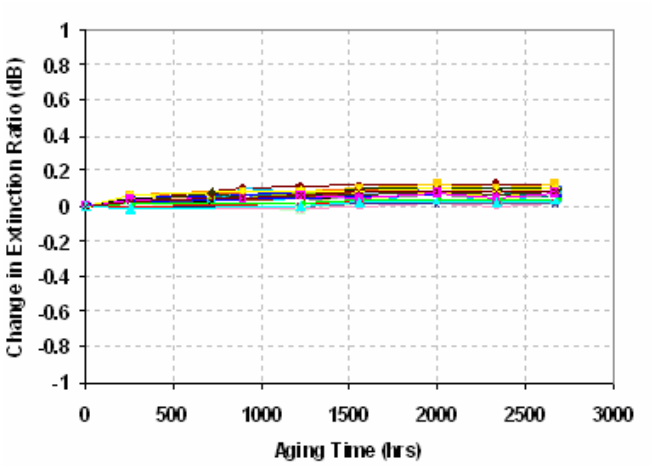

Fig. 13: Stress matrix to assess mirror aging. Sample size is 140 devices from 5 production wafers.

The modulator extinction ratio does not show any degradation. From the various tests performed we infer a modulator lifetime of more than 180 years. The estimated FIT rate is less than 100 over the expected normal operating time of the device.

Environmental Stability

Several environmental stability tests have been performed on chip, package, and transmitter module level in order to assess the reliability of the product according to Telcordia quality requirements. All the tests have demonstrated the excellent reliability of the tunable laser. One advantage of the monolithic integration scheme is the high degree of mechanical stability is provides. As an example we show the power in wavelength stability of the packaged tunable laser after going through mechanical vibration and shock testing in Fig. 14.

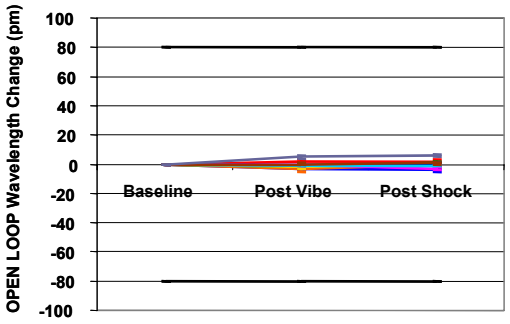

Fig. 14: Stability of output power in mechanical vibration and shock testing. Sample size 11 units.

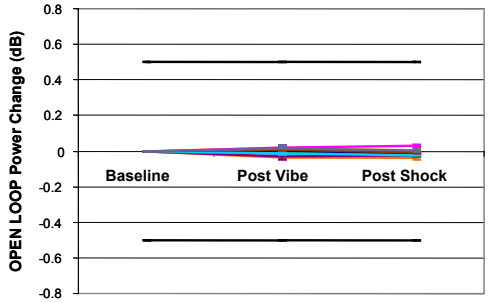

Fig. 15: Same devices as in Fig. 14. Stability of emission wavelength through mechanical vibration and shock testing.

The devices show excellent stability in all the mechanical tests performed. Since the wavelength tuning is achieved by electronic current injection and no mechanically moving parts are involved, the stability of the tunable laser transmitter is equivalent to standard fixed wavelength laser.

Conclusions

In conclusion, we have discussed the performance and reliability of widely tunable SG-DBR laser diodes with an integrated semiconductor optical amplifier. The cw output power of the packaged device is over 20mW. The wavelength tuning range spans the entire C- and L-band, respectively. The optical amplifier boosts the power level and provides a convenient way of power leveling.

The integrated, high speed modulator in the EML device is based on the Franz-Keldysh effect and achieves a large extinction ratio of more than 10dB. The time averaged output power is higher than 5dBm. Error free data transmission at a 2.5Gbit/s data rate (OC-48) is achieved over 350km of standard single mode fiber.

The tunable SG-DBR laser and the integrated electro-absorption modulator exhibit excellent reliability figures. The expected lifetime is over 100 years and the estimated failure rate is less than 100 FIT over the expected operating time of the device. The results demonstrate that SG-DBR lasers exhibit no reliability penalty for the wavelength tuning function. The devices are becoming key components in the next generation optical network systems.

References

1. D. Arent, A. Martin, “Third-generation DWDM networks near reality”, Lightwave by PennWell Corp., March 2001.
2. R. Dhar, M. Lowry, “Tunable lasers create dynamic networking capabilities”, WDM Solutions, pp. 83-88, Sept. 2001.
3. Y. A. Akulova, G. A. Fish, C. Schow, M. Larson, T. Liljeberg, A. Karim, E. Hall, T. Wipiejewski, D. Pavinski, T. Butrie, L. Coldren, “Widely-Tunable Electroabsorption-Modulated Sampled Grating DBR Laser”, Proc. IEEE LEOS 14th Annual Meeting, pp. 101-102, Nov. 2001
4. Y. A. Akulova, C. Schow, A. Karim, S. Nakagawa, P. Kozodoy, G. A. Fish, J. DeFranco, A. Dahl, M. Larson, T. Wipiejewski, D. Pavinski, T. Butrie, L. A. Coldren, “Widely-Tunable Electroabsorption-Modulated Sampled Grating DBR Laser Integrated with Semiconductor Optical Amplifier”, Proc. OFC, pp. 536-537, March 2002.
5. T. Wipiejewski, Y. A. Akulova, C. Schow, A. Karim, S. Nakagawa, P. Kozodoy, G. A. Fish, J. DeFranco, A. Dahl, M. Larson, D. Pavinski, T. Butrie, L. A. Coldren, “Monolithic Integration of a Widely Tunable Laser Diode with a High Speed Electro Absorption Modulator”, Proc. 52nd ECTC, San Diego, May 2002.
6. T. Wipiejewski, Y.A. Akulova, G.A. Fish, C. Schow, P. Koh, A. Karim, S. Nakagawa, A. Dahl, P. Kozodoy, A. Matson, B. Short, C. Turner, S. Penniman, M. Larson, C. Coldren, L.A. Coldren, “Integration of Active Optical Components”, Proc. SPIE Photonics West, Photonics Packaging and Integration V, San Jose, Jan. 2003.
7. V. Jayaraman, Z.-M. Chuang, L. A. Coldren, “Theory, Design, and Performance of Extended Tuning Range Semiconductor Laser with Sampled Grating”, IEEE J. of Quantum Electron., vol. 29, pp. 1824 –1834, 1993.
8. G.A. Fish, **“**Monolithic, widely-tunable, DBR lasers**”**, Optical Fiber Communication Conference and Exhibit, 2001, Volume: 2 , March 2001, pp. TuB1-2 -TuB1-4.
9. M.C. Larson, M. Bai, D. Bingo, N. Ramdas, S. Penniman, G.A. Fish, L A. Coldren, “Mode Control of Widely-Tunable SG-DBR Lasers”, Proc. ECOC, paper P2.4, Kopenhagen, Sep. 2002.
10. M.C. Larson, Y.A. Akulova, C. Coldren, T. Liljeberg, G.A. Fish, S. Nakagawa, A. Dahl, P. Kozodoy, D. Bingo, M. Bao, N. Ramadas, S. Penniman, T. Wipiejewski, L.A. Coldren, “High Performance Widely-Tunable SG-DBR Lasers”, Proc. SPIE Photonics West, Novel In-Plane Semiconductor Lasers V, San Jose, Jan. 2003.
11. D. Derickson, “Fiber Optics Test and Measurements,” Upper Saddle River, NJ: Prentice Hall PTR, p. 194, 1998.
12. Y. A. Akulova, G. A. Fish, P. C. Koh, C. Schow, P. Kozodoy, A. Dahl, S. Nakagawa, M. Larson, M. Mack, T. Strand, C. Coldren, E. Hegblom, S. Penniman, T. Wipiejewski, and L. A. Coldren**,** “Widely-Tunable Electroabsorption-Modulated Sampled Grating DBR Laser Transmitter”, to be published in JSTQE, 2002.
13. F. Delorme, G. Terol, H. de Baillieencourt, S. Grosmaire, P. Devoldere, “Long-tern wavelength stability of 1.55 -μm tunable distributed Bragg reflector lasers,” IEEE Journal of Selected Topics in Quantum Electronics, **5**(3), 480-6, 1999.
14. D.A. Ackerman, J.E. Johnson, George Chu Sung Nee, Zhang Liming, E.J. Dean, L.J.-P. Ketelsen, “Assessment and modeling of aging in electro-absorption distributed Bragg reflector lasers”, IEEE J. Quantum Electron., vol. 37, pp. 1382 –1387, 2001.
15. F. Delorme, B. Pierre, H. de Baillieencourt, G. Terol, and P. Devoldere, “Wavelength Aging Analysis of DBR Lasers Using Tuning Section IM Frequency Response Measurements”, IEEE Photon. Technol. Lett., vol. 11, pp. 310 –312, 1999.
16. H. Mawatari, M. Fukuda, F. Kano, Y. Tohmori, Y. Yoshikuni, H. Toba, “Lasing Wavelength Changes Due to Degradation in Buried Heterostructure Distributed Bragg Reflector Lasers”, J. Lightwave Technol., vol. 17, pp. 918 –923, 1999.